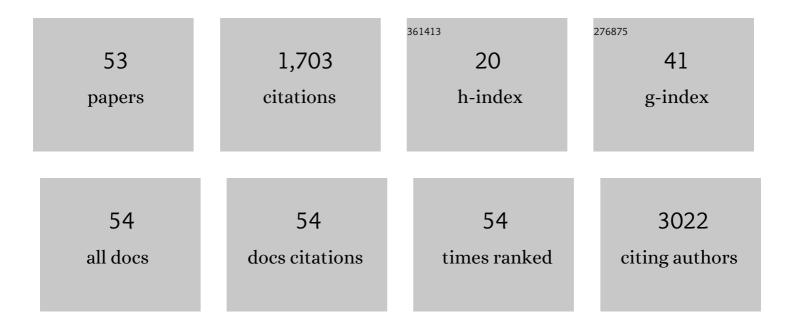
Yaakov R Tischler

List of Publications by Year in descending order

Source: https://exaly.com/author-pdf/1444953/publications.pdf Version: 2024-02-01



#	Article	IF	CITATIONS
1	CVD-Assisted Synthesis of 2D Layered MoSe ₂ on Mo Foil and Low Frequency Raman Scattering of Its Exfoliated Few-Layer Nanosheets on CaF ₂ Substrates. ACS Omega, 2022, 7, 4121-4134.	3.5	5
2	Identification of Enantiomers Using Low-Frequency Raman Spectroscopy. Analytical Chemistry, 2022, 94, 3188-3193.	6.5	3
3	Vibrational Strong Light–Matter Coupling in an Open Microcavity Based on Reflective Germanium Coatings. Journal of Physical Chemistry A, 2022, 126, 1282-1288.	2.5	2
4	Sulfur Treatment Passivates Bulk Defects in Sb ₂ Se ₃ Photocathodes for Water Splitting. Advanced Functional Materials, 2022, 32, .	14.9	18
5	Combining polarized low-frequency Raman with XRD to identify directional structural motifs in a pyrolysis precursor. Chemical Communications, 2021, 57, 7015-7018.	4.1	3
6	Higher Ultrasonic Frequency Liquid Phase Exfoliation Leads to Larger and Monolayer to Few-Layer Flakes of 2D Layered Materials. Langmuir, 2021, 37, 4504-4514.	3.5	21
7	Microcavity Enhanced Raman Spectroscopy of Fullerene C60 Bucky Balls. Sensors, 2020, 20, 1470.	3.8	4
8	New aqueous energy storage devices comprising graphite cathodes, MXene anodes and concentrated sulfuric acid solutions. Energy Storage Materials, 2020, 32, 1-10.	18.0	32
9	Raman scattering obtained from laser excitation of MAPbI3 single crystal. Applied Materials Today, 2020, 19, 100571.	4.3	2
10	Direct Formation of Carbocyanine J-Aggregates in Organic Solvent. Journal of Physical Chemistry C, 2019, 123, 19087-19093.	3.1	2
11	Polarization Dependence of Low-Frequency Vibrations from Multiple Faces in an Organic Single Crystal. Crystals, 2019, 9, 425.	2.2	5
12	Microcavity enhancement of lowâ€frequency Raman scattering from a CsPbI 3 thin film. Journal of Raman Spectroscopy, 2019, 50, 1672-1678.	2.5	4
13	Improving Raman spectra of pure silicon using super-resolved method. Journal of Optics (United) Tj ETQq1 1 0.78	4314 rgB1 2.2	「 /Overlock 1 21
14	Structural Characterization and Room Temperature Low-Frequency Raman Scattering from MAPbI3 Halide Perovskite Films Rigidized by Cesium Incorporation. ACS Applied Energy Materials, 2018, 1, 6707-6713.	5.1	20
15	Chiral Purity of Crystals Using Lowâ€Frequency Raman Spectroscopy. ChemPhysChem, 2018, 19, 3116-3121.	2.1	15
16	Characterization of peptides self-assembly by low frequency Raman spectroscopy. RSC Advances, 2018, 8, 16161-16170.	3.6	9
17	Deposition and Characterization of Roughened Surfaces. Langmuir, 2017, 33, 1810-1815.	3.5	5
18	Low Cost Method for Generating Periodic Nanostructures by Interference Lithography Without the Use of an Anti-Reflection Coating. MRS Advances, 2017, 2, 927-932.	0.9	0

YAAKOV R TISCHLER

#	Article	IF	CITATIONS
19	Microcavity Laser Based on a Single Molecule Thick High Gain Layer. ACS Nano, 2017, 11, 4514-4520.	14.6	11
20	New Method to Study the Vibrational Modes of Biomolecules in the Terahertz Range Based on a Single-Stage Raman Spectrometer. ACS Omega, 2017, 2, 1232-1240.	3.5	24
21	The effect of excitation wavelength and metallic nanostructure on SERS spectra of C ₆₀ . Journal of Raman Spectroscopy, 2017, 48, 829-836.	2.5	9
22	Characterization of Crystal Chirality in Amino Acids Using Low-Frequency Raman Spectroscopy. Journal of Physical Chemistry A, 2017, 121, 7882-7888.	2.5	21
23	Vibrational Strong Light–Matter Coupling Using a Wavelength-Tunable Mid-infrared Open Microcavity. Journal of Physical Chemistry C, 2017, 121, 18845-18853.	3.1	24
24	Replacing a Century Old Technique – Modern Spectroscopy Can Supplant Gram Staining. Scientific Reports, 2017, 7, 3810.	3.3	18
25	Influence of gain material concentration on an organic DFB laser. Optical Materials Express, 2016, 6, 2715.	3.0	2
26	Solid-State Rhodamine 6G Microcavity Laser. IEEE Photonics Technology Letters, 2016, 28, 1823-1826.	2.5	13
27	Strong Light-Matter Coupling and Hybridization of Molecular Vibrations in a Low-Loss Infrared Microcavity. Journal of Physical Chemistry Letters, 2016, 7, 2002-2008.	4.6	69
28	Strong lightâ€matter coupling between a molecular vibrational mode in a PMMA film and a lowâ€loss midâ€lR microcavity. Annalen Der Physik, 2016, 528, 313-320.	2.4	29
29	Third-Order Optical Nonlinearities in Organometallic Methylammonium Lead Iodide Perovskite Thin Films. ACS Photonics, 2016, 3, 361-370.	6.6	140
30	Spectroscopic Method for Fast and Accurate Group A Streptococcus Bacteria Detection. Analytical Chemistry, 2016, 88, 2164-2169.	6.5	13
31	A simplified method for generating periodic nanostructures by interference lithography without the use of an anti-reflection coating. Applied Physics Letters, 2015, 107, .	3.3	6
32	Photoinduced Reversible Structural Transformations in Free-Standing CH ₃ NH ₃ PbI ₃ Perovskite Films. Journal of Physical Chemistry Letters, 2015, 6, 2332-2338.	4.6	190
33	Room Temperature Fabrication of Dielectric Bragg Reflectors Composed of a CaF ₂ /ZnS Multilayered Coating. ACS Applied Materials & Interfaces, 2015, 7, 474-481.	8.0	30
34	Super-Resolved Raman Spectra of Toluene and Toluene–Chlorobenzene Mixture. Spectroscopy Letters, 2015, 48, 431-435.	1.0	12
35	Utilizing Pulsed Laser Deposition Lateral Inhomogeneity as a Tool in Combinatorial Material Science. ACS Combinatorial Science, 2015, 17, 209-216.	3.8	22
36	Synthesis and characterization of a J-aggregating TDBC derivative in solution and in Langmuir–Blodgett films. Journal of Luminescence, 2015, 158, 376-383.	3.1	8

YAAKOV R TISCHLER

#	Article	IF	CITATIONS
37	Fabrication of dielectric Bragg reflectors composed of CaF2 and ZnS for delicate lasing materials. , 2015, , .		1
38	Multiprobe NSOM fluorescence. Nanophotonics, 2014, 3, 117-124.	6.0	4
39	Reduced lasing threshold from organic dye microcavities. Physical Review B, 2014, 90, .	3.2	20
40	Millimeter-Tall Carpets of Vertically Aligned Crystalline Carbon Nanotubes Synthesized on Copper Substrates for Electrical Applications. Journal of Physical Chemistry C, 2014, 118, 19345-19355.	3.1	20
41	Raman and Photoluminescence Properties of Red and Yellow Rubrene Crystals. Journal of Physical Chemistry C, 2014, 118, 14528-14533.	3.1	11
42	Quantum Efficiency and Bandgap Analysis for Combinatorial Photovoltaics: Sorting Activity of Cu–O Compounds in All-Oxide Device Libraries. ACS Combinatorial Science, 2014, 16, 53-65.	3.8	83
43	Synthesis of an amphiphilic rhodamine derivative and characterization of its solution and thin film properties. Thin Solid Films, 2014, 564, 86-91.	1.8	6
44	Basic model of absorption depth and injection levels in silicon under intermediate illumination levels. Optics Communications, 2013, 291, 1-6.	2.1	3
45	Resonant Cavity Colloidal Quantum Dot LEDs. , 2011, , .		1
46	Efficient Förster energy transfer from phosphorescent organic molecules to J-aggregate thin films. Chemical Physics Letters, 2010, 485, 243-246.	2.6	12
47	Synthesis of J-Aggregating Dibenz[<i>a</i> , <i>j</i>]anthracene-Based Macrocycles. Journal of the American Chemical Society, 2009, 131, 5659-5666.	13.7	79
48	Electrostatic Formation of Quantum Dot/J-aggregate FRET Pairs in Solution. Journal of Physical Chemistry C, 2009, 113, 9986-9992.	3.1	76
49	Solid state cavity QED: Strong coupling in organic thin films. Organic Electronics, 2007, 8, 94-113.	2.6	104
50	Highly efficient resonant coupling of optical excitations in hybrid organic/inorganic semiconductor nanostructures. Nature Nanotechnology, 2007, 2, 555-559.	31.5	165
51	Critically coupled resonators in vertical geometry using a planar mirror and a 5 nm thick absorbing film. Optics Letters, 2006, 31, 2045.	3.3	136
52	Highly Efficient Blue Electroluminescence from Poly(phenylene ethynylene) via Energy Transfer from a Hole-Transport Matrix. Advanced Materials, 2005, 17, 1981-1985.	21.0	70
53	Layer-by-Layer J-Aggregate Thin Films with a Peak Absorption Constant of 106 cm–1. Advanced Materials, 2005, 17, 1881-1886.	21.0	99